

Absence of Biallelic TCR γ Deletions Predicts Early Treatment Failure in Pediatric T-Cell

Acute Lymphoblastic Leukemia

Gutierrez, et al.

SUPPLEMENTAL METHODS

Patient samples

Diagnostic specimens were collected with informed consent and institutional review board approval from pediatric patients with newly diagnosed T-ALL who were treated on Children's Oncology Group study P9404 (COG P9404) and Dana-Farber Cancer Institute study 00-01 (DFCI 00-01) for the initial data set,^{1,2} which rely on a nearly identical chemotherapy backbone including postinduction consolidation with asparaginase and doxorubicin, which has contributed to long-term event-free survival rates of 75%.³ Cases treated on studies COG AALL0434 and DFCI 05-01 were used for the first validation data set.⁴⁻⁶ Induction chemotherapy regimens for all studies in this manuscript are summarized in Supplemental Table 2. Events on these clinical trials were defined as induction failure, relapse, death, or second malignancy, but we limited our analyses to cases whose event was induction failure or relapse.

Response to induction chemotherapy was assessed by examining the bone marrow, peripheral blood, and central nervous system for evidence of persistent leukemia, four weeks following the start of multi-agent induction chemotherapy. Complete remission was defined as <5% lymphoblasts in the bone marrow with no evidence of peripheral blood, central nervous system, or extramedullary leukemia, in the setting of hematologic recovery (defined as a bone marrow biopsy showing trilineage hematopoiesis; on DFCI 00-01 and 05-01, hematologic recovery additionally required a peripheral blood absolute phagocyte count $\geq 1,000/\text{mm}^3$ and platelet count $\geq 100,000/\text{mm}^3$). Patients failing to achieve complete remission were classified

as induction failure if they had a high fraction of lymphoblasts in the bone marrow 4 weeks following the start of combination chemotherapy (>25% on COG P9404 and AALL0434; >15% on DFCI 00-01 and 05-01). Patients that failed to meet complete remission criteria but that had low or intermediate levels of lymphoblasts in the bone marrow were followed with weekly bone marrow aspirates and biopsies on studies COG P9404, DFCI 00-01, and DFCI 05-01; failure to achieve <5% lymphoblasts in the bone marrow by week 6 from the start of combination chemotherapy was defined as induction failure on these studies. COG AALL0434 patients with 5-25% blasts or with minimal residual disease \geq 1% by flow cytometry at the end of induction were assigned to the high-risk group but were not included in the induction failure group. Note that minimal residual disease levels \geq 1% at the end of induction chemotherapy for T-ALL have been associated with outcomes nearly as poor as those of patients with induction failure, with an estimated 5-year relapse-free survival rate of only 14%.⁷ Cases of relapse were those in which induction chemotherapy successfully induced a complete remission, but disease recurrence occurred at a later time point. Event-free survivors were patients that achieved complete remission and had no evidence of later disease recurrence. The event time for induction failure cases was defined at time zero on DFCI clinical trials, whereas it was defined at the time between the initiation of therapy and the performance of the study diagnostic for induction failure on COG clinical trials; there were no other differences in event-free or overall survival measurements between these trials.

Mononuclear cells were purified from diagnostic bone marrow or peripheral blood specimens by Ficoll-Paque centrifugation according to the manufacturer's instructions (GE Healthcare, Piscataway, NJ) prior to cryopreservation. All specimens analyzed consisted of greater than 90% lymphoblasts. Genomic DNA was extracted with the PureGene kit or the DNeasy blood & tissue kit according to the manufacturer's instructions (Qiagen Inc, Valencia,

CA), as previously described.⁸ Samples initially extracted with the PureGene kit were repurified with the DNeasy kit prior to array CGH analysis.

ABD was also validated in a second independent data set consisting of children with T-ALL treated on St. Jude Total Therapy Studies 13A to 15,^{9,10} whose TCR γ status was previously assessed by SNP array analysis.^{11,12} Response to the initial phase of St. Jude induction chemotherapy was assessed by flow cytometric assessment of a bone marrow specimen for residual leukemic cells at day 19 of induction, as described.^{9,10} An inadequate response to the first phase of induction on these clinical trials was defined as $\geq 1\%$ residual leukemic cells in the bone marrow at this time point.

Matched specimens of lymphoblasts collected at diagnosis and at the time of relapse from the same patients were collected as previously described.^{11,13}

Array CGH

Microarray-based array comparative genomic hybridization (array CGH) was performed using genomic DNA on Agilent Human Genome CGH 244A Microarrays (Agilent Technologies, Santa Clara, CA) as previously described.^{8,14} Pooled DNA from 7 healthy males (Promega, Madison, WI) was used as the CGH control. Feature extraction data were obtained using Agilent G2567AA Feature Extraction Software, normalized using a LOWESS R package developed by Dr. Lynda Chin's laboratory (http://genomic.dfci.harvard.edu/Tools/Agilent_1.0.2.tar.gz), and then subjected to circular binary segmentation using the DNACopy package of the BioConductor project (<http://www.bioconductor.org/packages/2.2/bioc/html/DNACopy.html>). Color plots of the segmented Log₂ copy number data were generated using dChip software (<http://biosun1.harvard.edu/complab/dchip>). Array CGH data are available on the GEO website under accession numbers GSE14959 and GSE7615 (see Table S1, sheet 2). Note that CGH quality controls failed on T-ALL samples 36 and 37, thus these were excluded from analysis. The CGH log₂ copy number ratio for heterozygous deletion was defined as -0.5 to -1.5

(corresponding to 35-70% of normal copy number), while log₂ copy number ratios lower than -1.5 (corresponding to less than 35% of normal copy number) were defined as homozygous deletions. The Agilent 244A CGH microarrays utilized harbor 3 probes within the TCR γ intron between the most 3' V pseudoexon (*TRGV11*) and the most 5' J exon (*TRGJP1*), which should be involved by any TCR γ locus deletion resulting from V-J recombination.

Note that we were unable to identify a combination of genetic alterations that was superior to ABD status alone.

Gene Abbreviations

TCR γ , T cell receptor γ locus, TRG@. TCR α , T cell receptor α locus, TRA@. TCR δ , T cell receptor δ locus, TRD@. TCR β , T cell receptor gene β , TRB@.

Statistical Methods

Differences in categorical data were assessed via Fisher's exact test, and differences in continuous data were assessed via the Mann-Whitney (rank-sum) test. Differences in event-free survival and overall survival were assessed by the log-rank test, and time-to-event distributions were estimated and plotted via the Kaplan-Meier method using R version 2.8.0 (<http://www.r-project.org>).

Quantitative DNA PCR for Absence of Biallelic TCR γ Deletions

Quantitative DNA PCR (Q-PCR) for TCR γ rearrangements was performed using primers targeting the intron between the most 3' V exon (V11) and the most 5' J exon (JP1) of the TCR γ (TRG@) gene, because this intron should be involved in any TCR γ deletion event resulting from V(D)J recombination. Control Q-PCR primers were located in the *ANLN* locus, located approximately 1.9 Mbp downstream of TCR γ at 7p15-14. There were no known single-

nucleotide polymorphisms in the sequences targeted by the Q-PCR primers in the dbSNP build 129, examined using the UCSC genome browser (<http://genome.ucsc.edu/>). Furthermore, none of the control genomic regions targeted by quantitative PCR were involved by known germline copy number alterations based on the Database of Genomic Variants (<http://projects.tcag.ca/variation/>).¹⁵ Quantitative DNA-PCR primer sequences were as follows: TCRG-VJ forward, CATCCTCACTTTCCTGCTTCTTC; TCRG-VJ reverse, CCAAGGTGAATCCCTACATGCT. ANLN forward, AAATTCTGCCCTTTGCTTGTTT; ANLN reverse, GAAAGCAACCACAGAGAATATGTAAGTAA.

Quantitative DNA PCR was performed using 50 ng of genomic DNA, 3 mcl of 1 micromolar primer, and 7.5 mcl of Power SYBR green mastermix (Applied Biosystems, Foster City, CA) in a total volume of 15 mcl per reaction, using an Applied Biosystems 7300 Real Time PCR System instrument. The Q-PCR reaction conditions were as follows: Initial denaturation step, 94°C x 10 min; Forty PCR cycles at 94°C x 10 secs, then 60 °C x 60 sec. Data was acquired at the end of each 60 °C step. All PCR reactions were performed in triplicate. PCR primer pairs were first tested using control germline DNA from 5 healthy individuals, collected anonymously from healthy volunteers by Scope oral rinse for 2 minutes. The cells were pelleted by centrifugation, washed x 2 with phosphate-buffered saline (Gibco), and genomic DNA was extracted using the PureGene kit (Qiagen) according to the manufacturer's instructions. Quantitative DNA PCR performed with 50 ng of this mouthwash DNA was used to test the relative efficiency of each primer pair, which demonstrated that the TCR γ -VJ primer pair had higher relative efficiency than the ANLN primer pair, consistently leading to detection of signal at 2.02 +/- 0.40 fold greater intensity than the ANLN PCR in control germline DNA. Therefore, a correction factor for differences in relative primer efficiency was applied to all future PCRs corresponding to a 2.02 fold change for TCR γ -VJ. Results of the TCR γ -VJ quantitative PCRs are reported as fold-change compared to the ANLN Q-PCR. The ANLN Q-PCR consistently

gave detectable signal in less than 25 Q-PCR cycles in all control samples tested, thus we considered the Q-PCR to have failed if the average ANLN PCR cycle count to detection was ≥ 25 . We also considered any Q-PCR to have failed if the standard deviation of the 3 replicates was ≥ 0.5 Q-PCR cycles. The threshold for a homozygous deletion call by Q-PCR was defined as fold-change < 0.35 (corresponding to $< 35\%$ of normal copy number).

Expression Microarray Analysis

Expression microarrays were previously performed on a subset of the cases analyzed using Affymetrix U133 Plus 2.0 arrays (Affymetrix, Santa Clara, CA), as previously described.² The expression profiling data are available in the NCBI gene expression omnibus under accession number GSE14618 (see Table S1, sheet 2). Expression data were extracted from CEL files using dChip 2007 software (<http://biosun1.harvard.edu/complab/dchip/>), and normalized to case T-ALL 15. The presence of the early T-cell precursor gene expression signature was assessed by hierarchical clustering using the gene expression probe list described by Coustan-Smith and colleagues, comprising 62 probe sets.¹⁶ Hierarchical clustering was performed using the HierarchicalClustering module of GenePattern (<http://www.broad.mit.edu/cancer/software/genepattern/index.html>),¹⁷ using the following parameters: Column distance measure, Pearson correlation; Row distance measure, No row clustering; Clustering method, Pairwise complete-linkage; Log transform, no; Row center, Subtract the mean of each row; Row normalize, yes; Column center, Subtract the mean of each column; Column normalize, yes. Gene set enrichment analysis was performed as previously described,^{18,19} using the gene sets from the Molecular Signatures Database (MSigDB) available online at the GSEA website (<http://www.broad.mit.edu/gsea/>).

Immunophenotyping

Immunophenotyping was performed at the clinical diagnostic laboratory used by each individual Children's Oncology Group or Dana-Farber Cancer Institute Acute Lymphoblastic Leukemia Consortium member institution. The definition of the early T-cell precursor (ETP) immunophenotype was as described by Coustan-Smith and colleagues: absent (<5%) CD1a and CD8, weak (<75%) CD5, and expression >75% of one or more of the following: CD117, CD34, HLA-DR, CD13, CD33, CD11b, or CD65.¹⁶

Mutation Detection

Sequencing was performed on the coding sequence of exons 26, 27 and 34 of *NOTCH1*, exons 9 and 10 of *FBXW7*, the entire coding region of *PTEN*, exons 9 and 20 of *PIK3CA* (encoding the catalytic subunit of class IA PI3K), exons 12 and 13 of *PIK3RA* (encoding the regulatory subunit of class IA PI3K), exon 2 of the *AKT1-3* genes, exons 1-2 of *NRAS* and *KRAS*, the entire coding sequence of *LEF1*, and exons 4-7 of *TP53*, as previously described.^{8,19} All sequencing was performed at Agencourt Bioscience Corporation, Beverly, MA.

SUPPLEMENTAL REFERENCES

1. DFCI 00-01 clinicaltrials.gov identifier: NCT00165178.
<http://clinicaltrials.gov/ct2/show/NCT00165178?term=NCT00165178&rank=1>.
2. Winter SS, Jiang Z, Khawaja HM, et al: Identification of genomic classifiers that distinguish induction failure in T-lineage acute lymphoblastic leukemia: a report from the Children's Oncology Group. *Blood* 110:1429-38, 2007
3. Goldberg JM, Silverman LB, Levy DE, et al: Childhood T-cell acute lymphoblastic leukemia: the Dana-Farber Cancer Institute acute lymphoblastic leukemia consortium experience. *J Clin Oncol* 21:3616-22, 2003
4. COG AALL0434 clinicaltrials.gov identifier: NCT00408005.
<http://clinicaltrials.gov/ct2/show/NCT00408005?term=winter+stuart+children%27s+oncology+group&rank=1>.
5. DFCI 05-01 clinicaltrials.gov identifier: NCT00400946.
<http://clinicaltrials.gov/ct2/show/NCT00400946?term=NCT00400946&rank=1>.
6. Silverman LB, Supko JG, Stevenson KE, et al: Intravenous PEG-asparaginase during remission induction in children and adolescents with newly diagnosed acute lymphoblastic leukemia. *Blood*, 2009
7. Willemse MJ, Seriu T, Hettinger K, et al: Detection of minimal residual disease identifies differences in treatment response between T-ALL and precursor B-ALL. *Blood* 99:4386-93, 2002
8. Gutierrez A, Sanda T, Grebliunaite R, et al: High frequency of PTEN, PI3K, and AKT abnormalities in T-cell acute lymphoblastic leukemia. *Blood* 114:647-50, 2009
9. Pui CH, Campana D, Pei D, et al: Treating childhood acute lymphoblastic leukemia without cranial irradiation. *N Engl J Med* 360:2730-41, 2009
10. Pui CH, Pei D, Sandlund JT, et al: Long-term results of St Jude Total Therapy Studies 11, 12, 13A, 13B, and 14 for childhood acute lymphoblastic leukemia. *Leukemia*, 2009
11. Mullighan CG, Phillips LA, Su X, et al: Genomic analysis of the clonal origins of relapsed acute lymphoblastic leukemia. *Science* 322:1377-80, 2008
12. Mullighan CG, Goorha S, Radtke I, et al: Genome-wide analysis of genetic alterations in acute lymphoblastic leukaemia. *Nature* 446:758-64, 2007
13. Tosello V, Mansour MR, Barnes K, et al: WT1 mutations in T-ALL. *Blood* 114:1038-45, 2009
14. Maser RS, Choudhury B, Campbell PJ, et al: Chromosomally unstable mouse tumours have genomic alterations similar to diverse human cancers. *Nature* 447:966-71, 2007
15. Iafrate AJ, Feuk L, Rivera MN, et al: Detection of large-scale variation in the human genome. *Nat Genet* 36:949-51, 2004
16. Coustan-Smith E, Mullighan CG, Onciu M, et al: Early T-cell precursor leukaemia: a subtype of very high-risk acute lymphoblastic leukaemia. *Lancet Oncol* 10:147-56, 2009
17. Reich M, Liefeld T, Gould J, et al: GenePattern 2.0. *Nat Genet* 38:500-1, 2006
18. Subramanian A, Tamayo P, Mootha VK, et al: Gene set enrichment analysis: a knowledge-based approach for interpreting genome-wide expression profiles. *Proc Natl Acad Sci U S A* 102:15545-50, 2005
19. Gutierrez A, Sanda T, Ma W, et al: Inactivation of LEF1 in T-cell acute lymphoblastic leukemia. *Blood*, in press

SUPPLEMENTAL FIGURE LEGENDS

Figure S1. Relation of *TCR β* deletions to treatment failure. (A) Array CGH data shown as a dChip plot of CGH segmented log₂ copy number ratios at the *TCR β* locus. Red arrows denote cases with absence of *TCR β* deletion. IF, induction failure. (B,C) Kaplan-Meier analysis of event-free and overall survival for T-ALL cases classified by *TCR β* deletion status. Tick marks indicate patients still at risk.

Figure S2. Relation of biallelic *TCR α/δ* deletions to treatment failure. (A) Array CGH data shown as a dChip plot of CGH segmented log₂ copy number ratios at the *TCR α/δ* locus. Red arrows denote cases with absence of biallelic *TCR α/δ* deletions. The green box denotes the location of the *TCR α* locus, while the red box denotes the location of the *TCR δ* locus. IF, induction failure. (B,C) Kaplan-Meier analysis of event-free and overall survival for T-ALL cases classified by the absence of biallelic *TCR α/δ* deletions. Tick marks indicate patients still at risk.

Figure S3. Relation of *CDKN2A* deletions to treatment failure. (A) Array CGH data shown as a dChip plot of CGH segmented log₂ copy number ratios at the *CDKN2A* locus. Red arrows denote cases with absence of biallelic *CDKN2A* deletion. IF, induction failure. (B,C) Kaplan-Meier analysis of event-free and overall survival for T-ALL cases classified by *CDKN2A* deletion status. Tick marks indicate patients still at risk.

Figure S4. Gene expression profiling was previously performed on 40 of the 47 T-ALL cases analyzed by array CGH using Affymetrix U133 Plus 2.0 microarrays. (A) Heatmap showing the expression pattern of known T-ALL oncogenes, based on the microarrays applied. Probe sets that demonstrated no significant expression (defined as expression values < 100) in any T-ALL

sample were excluded. Low expression values were truncated to 30. Note that data from the [1561651_s_at] *TAL1* probeset were excluded because we have found that expression measured by this probeset does not correlate with *TAL1* RNA levels (data not shown). (B-C) ABD T-ALLs were characterized by increased expression of *LYL1* and *ERG*, features previously associated with ETP T-ALL.¹⁶ (D) ETP T-ALL cases were previously found to have an increased number of copy number alterations by SNP array,²³ but we found no such association with ABD T-ALL. (E-G) Gene set enrichment analysis (GSEA) revealed that gene expression in ABD T-ALL showed significant similarity to that of gastric cancer cells in which cisplatin resistance was experimentally induced, as well as increased expression of genes within the PI3K-PIP3-AKT and RAF-MEK-ERK signal transduction pathways.

Figure S5. Copy number at the *TCR γ* locus was assessed by SNP array (A) or Q-PCR analysis (B) in a set of T-ALL samples collected at diagnosis and relapse from the same patients. Twenty-six of the T-ALL cases analyzed harbored biallelic *TCR γ* deletions at diagnosis, and 5 of these relapsed as ABD (red boxes), indicating that the subclone responsible for relapse showed T cell developmental arrest prior to biallelic *TCR γ* recombination, earlier than the majority of blasts at diagnosis.

SUPPLEMENTAL FIGURES

Figure S1. TCR β

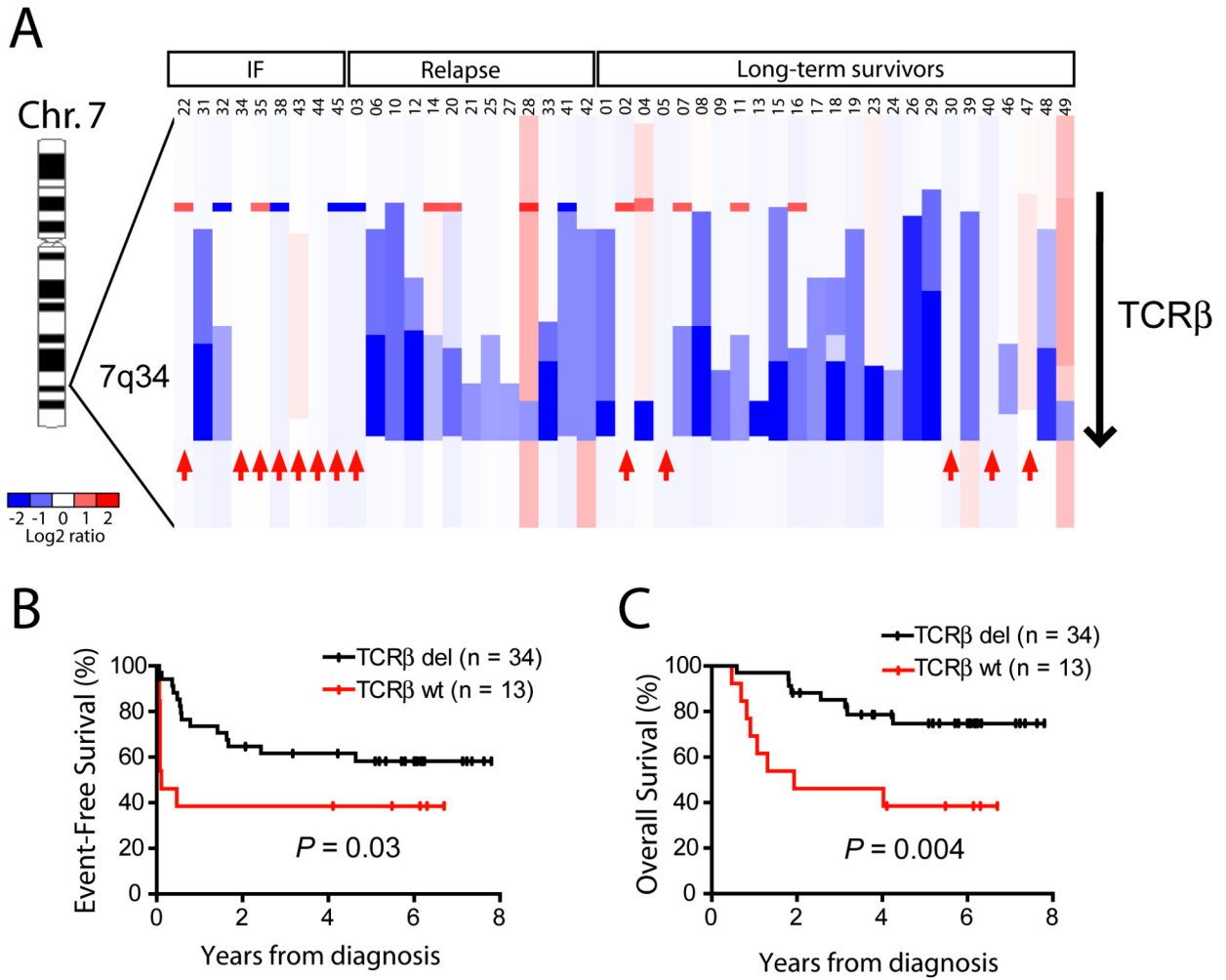


Figure S2. TCR α/δ

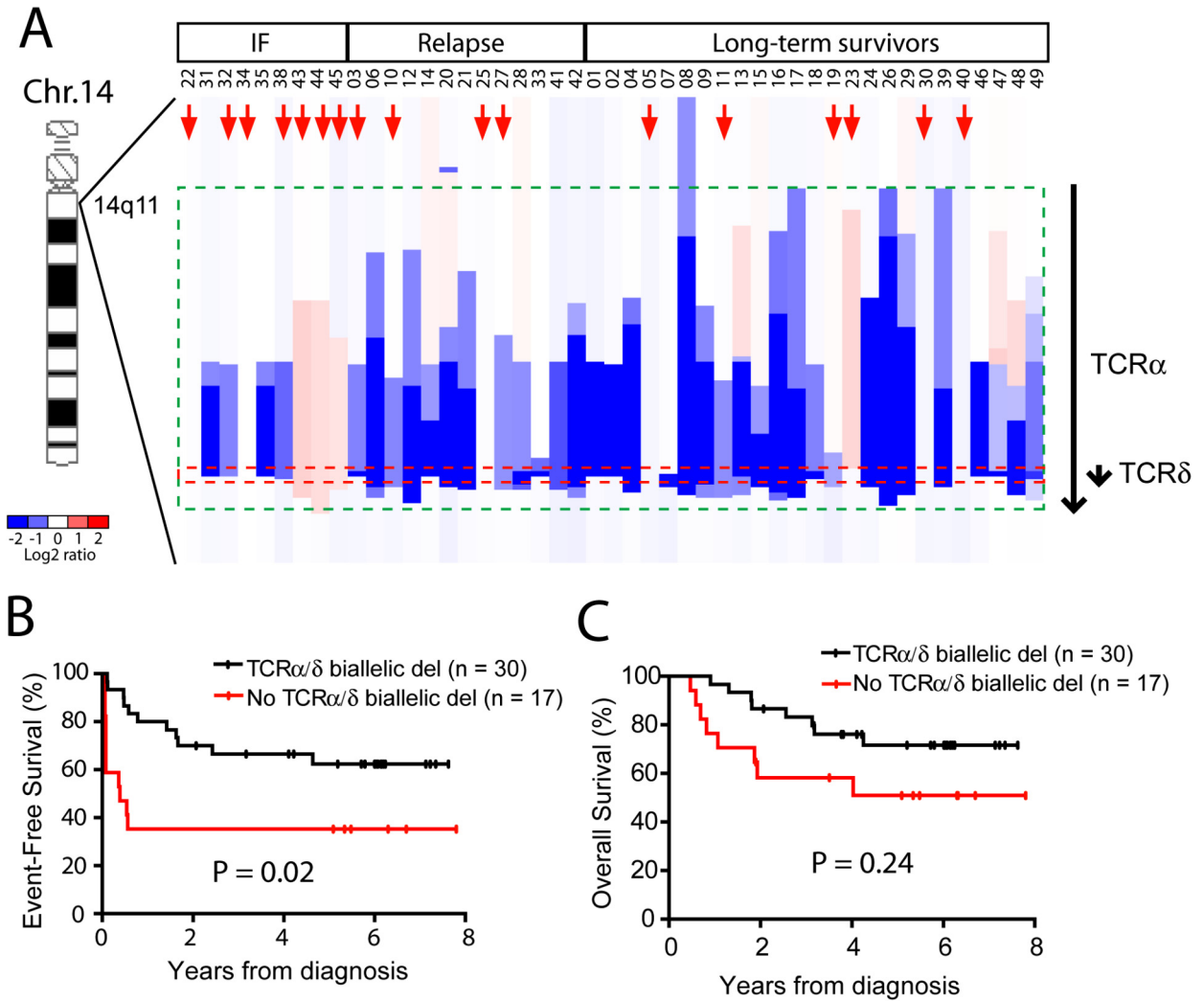


Figure S3. CDKN2A

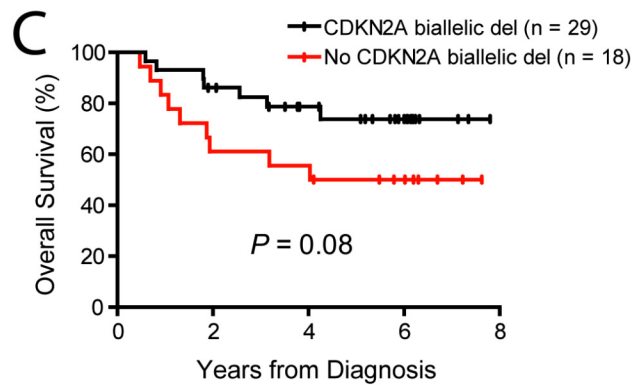
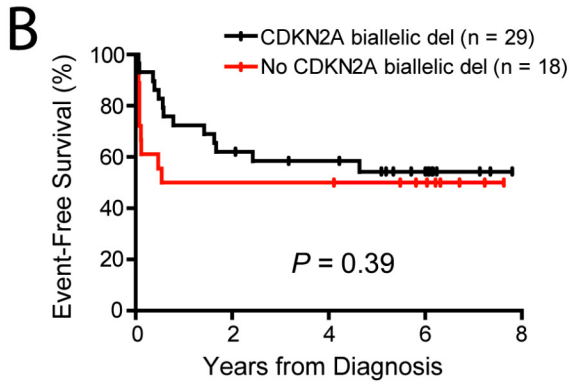
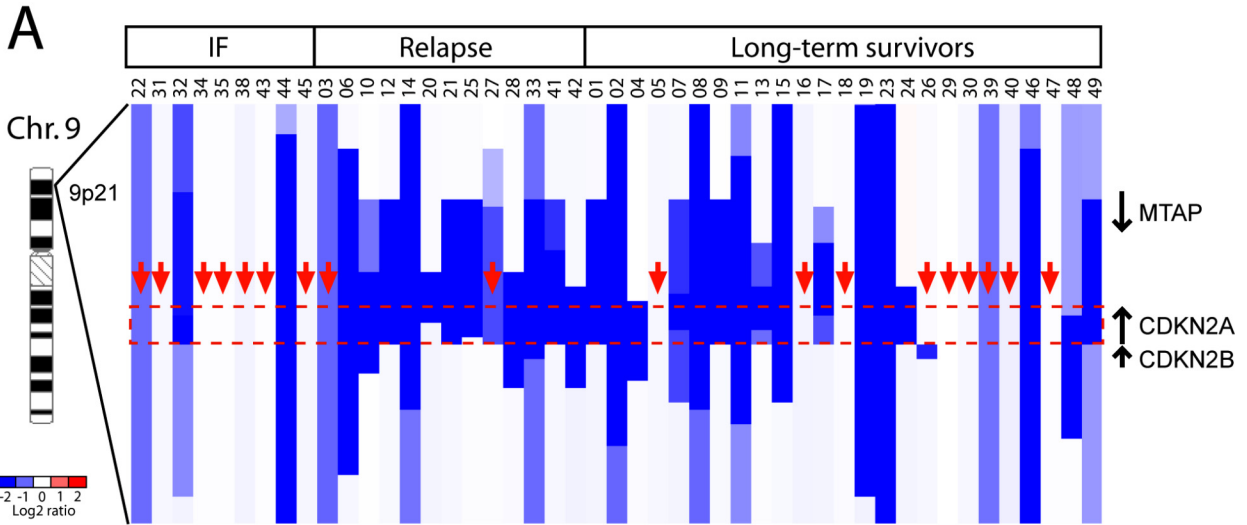


Figure S4

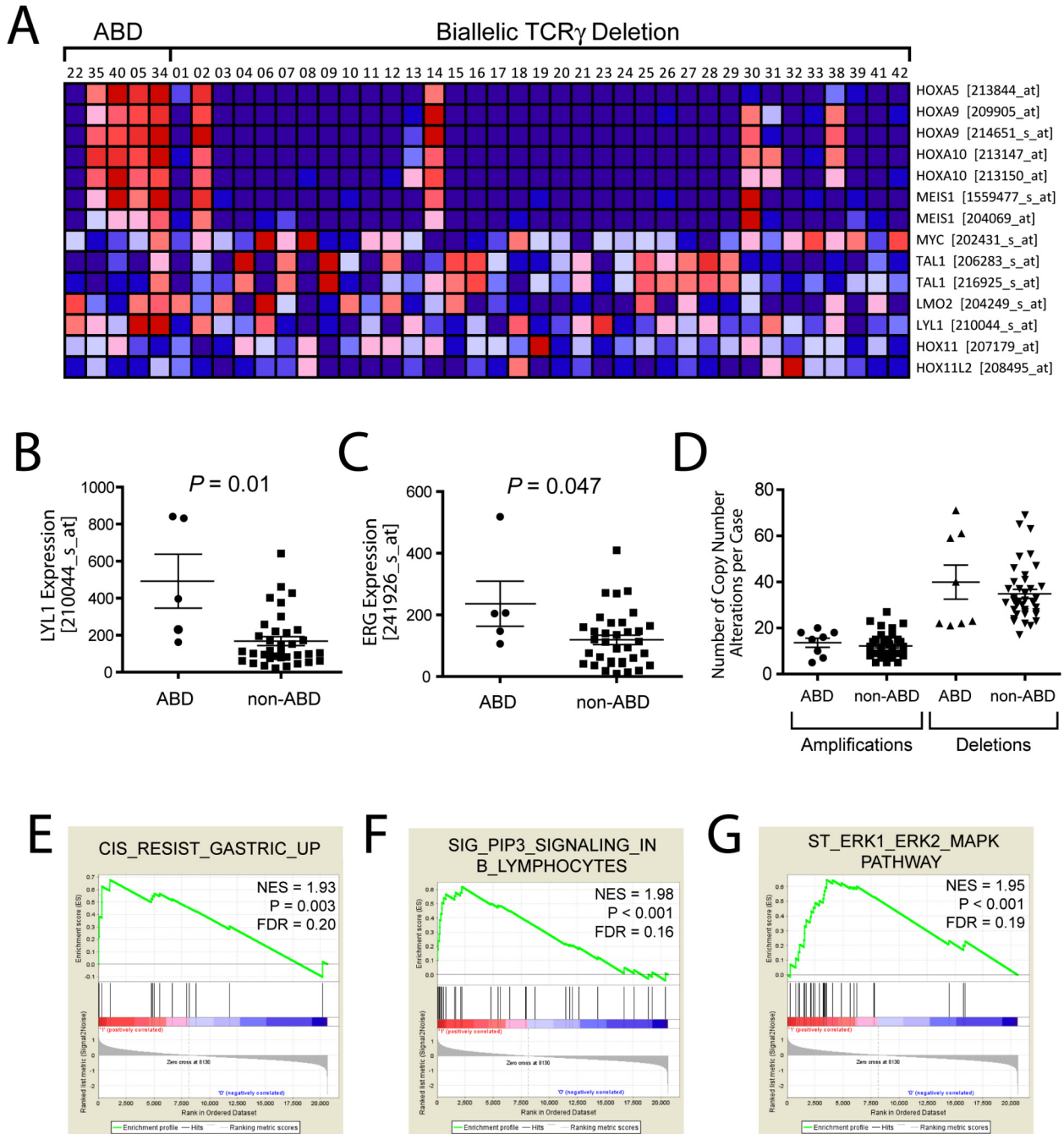


Figure S5

